

High injection rates counteract formation of far-reaching fluid migration pathways at The Geysers geothermal field

Stanislaw Lasocki^{1,1} and Beata Orlecka-Sikora^{2,2}

¹Institute of Geophysics, Polish Academy of Sciences

²Institute of Geophysics Polish Academy of Sciences

November 30, 2022

Abstract

Deep underground water injections induce seismicity. When the seismic fractures coalesce into far-reaching pathways for fluid migration, the migrating fluid may reach pre-existing faults, and by decreasing fault strength, can trigger major seismic events. We assume that the potential for building such pathways depends on closeness of hypocenters, similarity of fracture planes orientations, and closeness of radii taking off from the injection point, on which events locate. We define this potential as the average distance between seismic events in the space of parameters quantifying the above conditions. We show that in the studied case from The Geysers geothermal field, this potential is highly correlated with injection rate. When the overall level of injection rate is high, the higher the injection rate, the more the potential for building far-reaching pathways for fluid migration is reduced.

Figure 1.

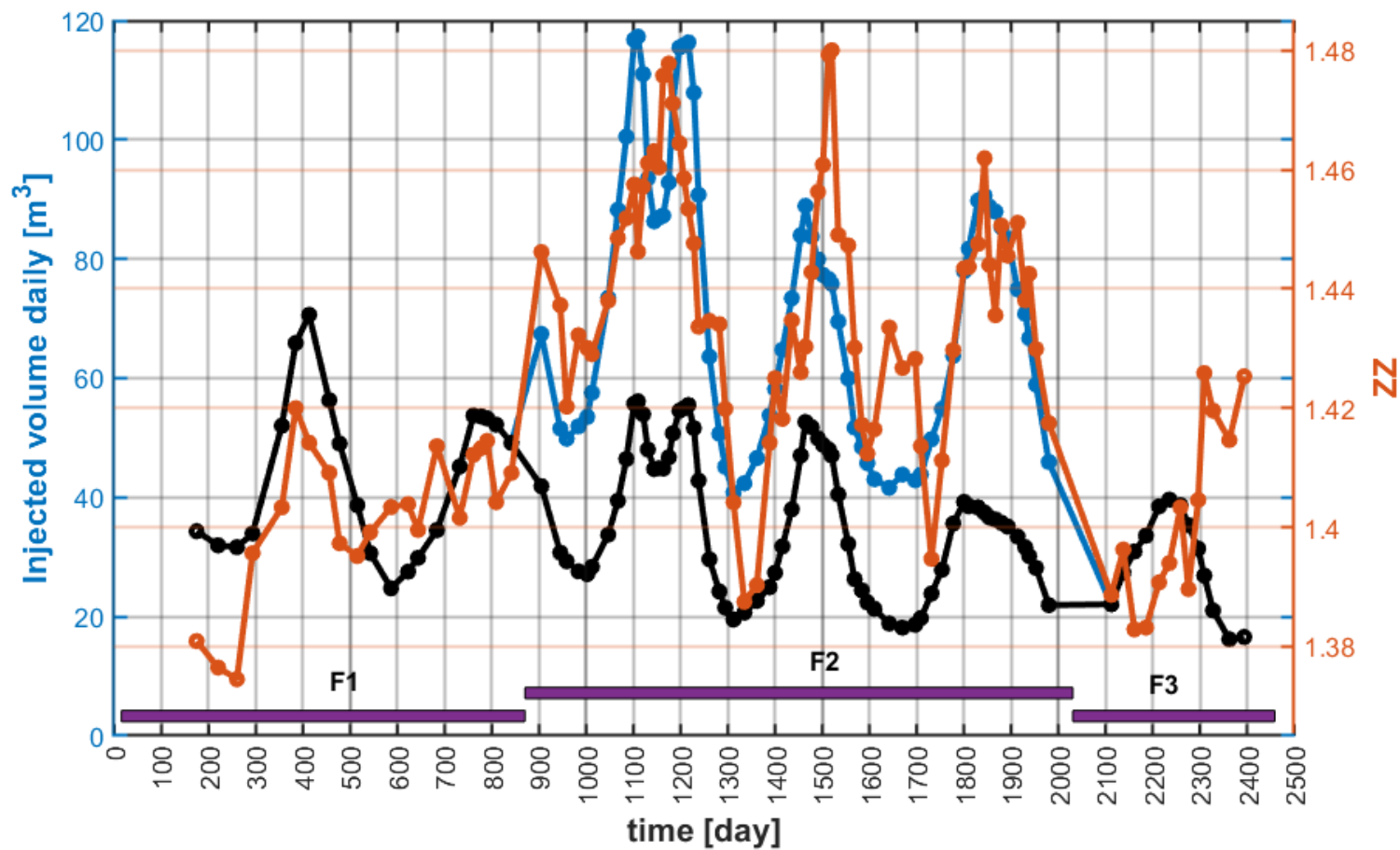
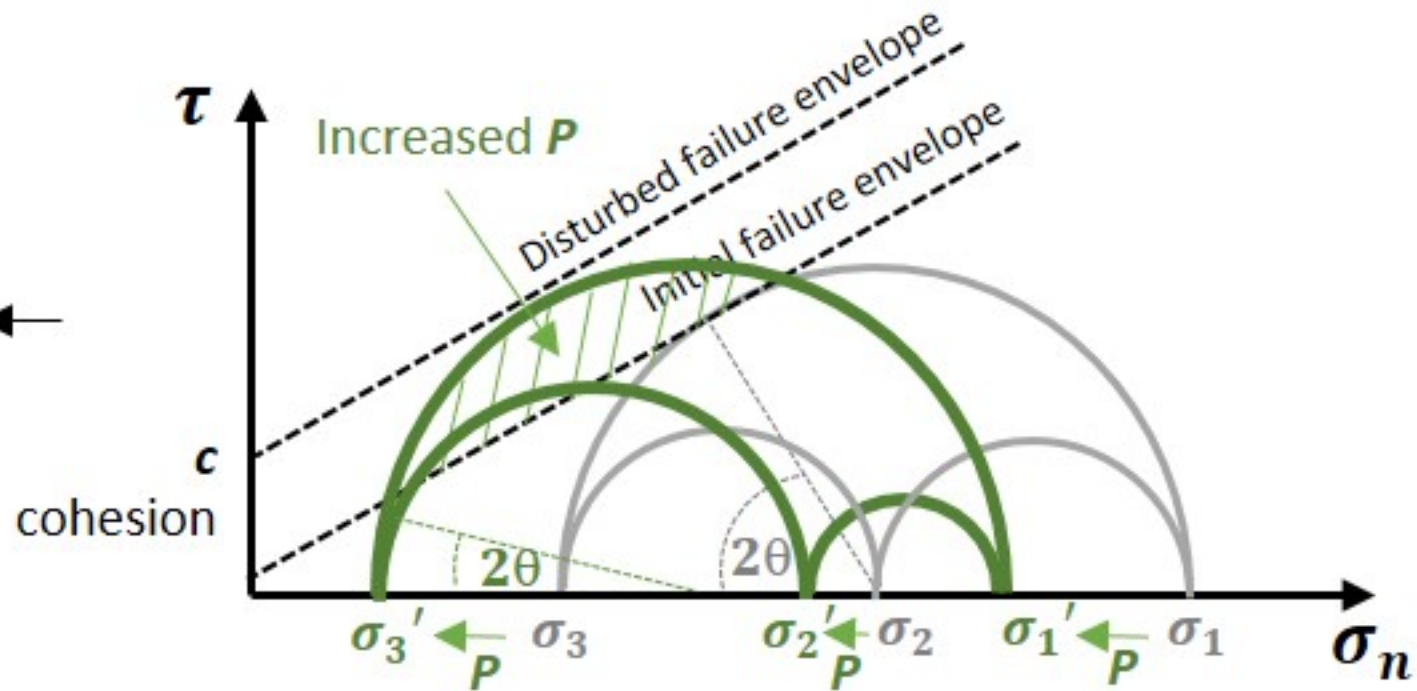
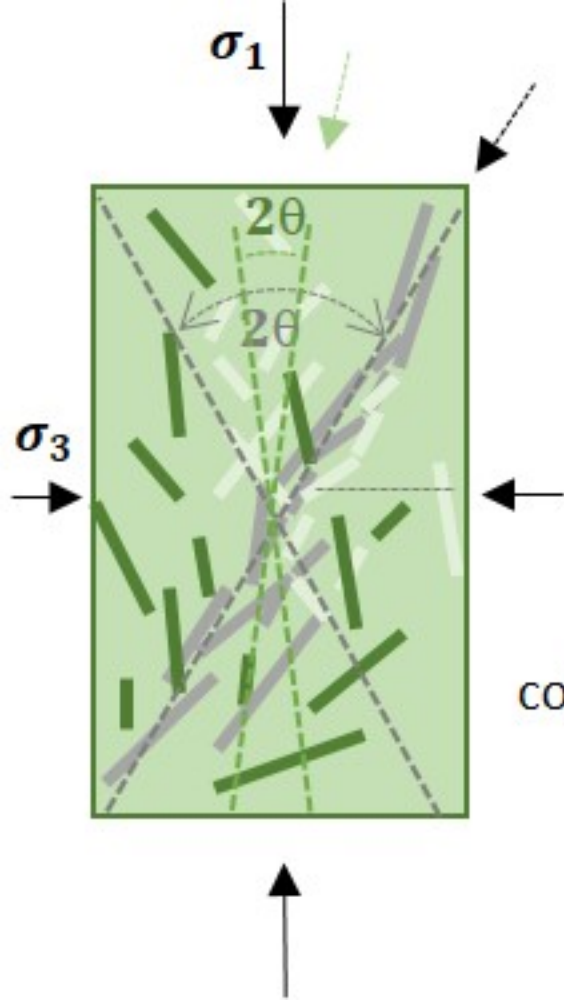


Figure 2.



**High injection rates counteract formation of far-reaching fluid migration pathways
at The Geysers geothermal field**

Stanisław Lasocki¹, and Beata Orlecka-Sikora¹

¹Institute of Geophysics Polish Academy of Sciences.

Corresponding author: Stanisław Lasocki (lasocki@igf.edu.pl)

Key Points:

- Degree of seismic sources disorder correlates with injection rate and amplitudes of its changes agree with injection rate changes.
- Formation of long pathways for fluid migration requires certain ordering of seismic sources.
- High injection rates increase sources disorder hence decrease chance for seismic fractures to coalesce into long fluid migration pathways.

Abstract

Deep underground water injections induce seismicity. When the seismic fractures coalesce into far-reaching pathways for fluid migration, the migrating fluid may reach pre-existing faults, and by decreasing fault strength, can trigger major seismic events. We assume that the potential for building such pathways depends on closeness of hypocenters, similarity of fracture planes orientations, and closeness of radii taking off from the injection point, on which events locate. We define this potential as the average distance between seismic events in the space of parameters quantifying the above conditions. We show that in the studied case from The Geysers geothermal field, this potential is highly correlated with injection rate. When the overall level of injection rate is high, the higher the injection rate, the more the potential for building far-reaching pathways for fluid migration is reduced.

Plain Language Summary

Geothermal energy production is often based on pumping cold water down to hot rocks and taking back steam. Pressurized underground water injections induce brittle fracturing of rocks, that is seismic events, what enhances the rock permeability and in this way increases the surface on which heat exchange takes place. However, the seismic fractures may also coalesce into undesired pathways enabling the fluids to migrate far and reach pre-existing tectonically preloaded faults. Then the fluids decrease fault strength, and in result the fault can rupture producing a major seismic event. We studied how some properties of the seismicity induced by injections of water in a part of the Geysers, which can lead to the mentioned undesired fracture network development, depend on injection rates. Our studies indicated that the potential for such network development is highly correlated with the injection rate. Moreover, it turned out that in order to avoid this unwanted development of fracture network the injection rates should be kept high. The higher the injection rate is, the more the potential for building far-reaching pathways for fluid migration is reduced. These results, when confirmed on other seismically active geothermal energy production cases can have important implications for strategies of geothermics.

1 Introduction

Deep underground water injections induce seismicity. This seismic fracturing of rocks is desirable as it increases the surface on which heat exchange takes place in Enhanced Geothermal Systems. However, the seismic fractures may also coalesce into undesired pathways for fluid migration. These are such pathways that enable the fluids to reach pre-existing faults. In result, by decreasing fault strength, the fluids can trigger ruptures and produce major seismic events. The further the migration pathways extend from the injection point, the more probable are these unwanted effects. It is therefore of paramount importance to recognize under which injection conditions an induced seismic process can produce such pathways (e.g.: Davies et al., 2013; Ellsworth, 2013; Majer et al., 2012; Zhang Dongxiao & Yang Tingyun, 2015).

Numerous studies indicate that the geometry of fractures and the structure of fracture networks are the main factors controlling fluid flow and the fluid transport characteristics of rocks (e.g.: Hope et al., 2015; Lee et al., 1990; Long & Billaus, 1987; Schwartz et al., 1983; Snow, 1965). The development of the fracturing process has been investigated in a number of laboratory experiments (e.g.: Ko & Kemeny, 2011; Lockner et al., 1992; Stanchits et al., 2006). Based on these experiments, many models have been developed to simulate the geometry of

fractures and the topology of fracture networks (e.g.: Hope et al., 2015; Lee et al., 1990; Long & Billaus, 1987). However, although seismic field data provide direct insight into the development of fracture networks at the crustal scale, there are few studies focused on this topic (e.g.: Chorozoglou et al., 2018; Kagan, 1992; 2000; Orlecka-Sikora et al., 2019; Sausse et al., 2010).

Here we study seismic and injection data from a part of the Geysers geothermal field to determine a relationship between the injection conditions and the potential of injection-induced seismicity to build far-reaching pathways for fluid migration. We formulate three conditions which we expect to play a role in linking fractures and building such pathways: closeness of hypocenters; similarity of fracture planes orientations; closeness of radii, which begin at the open hole section of the injection well and on which events occur. We assume that in the same injection conditions and for the same orientation of the line connecting hypocenters of two events with respect to the orientation of regional stress field, the probability for these events to link is higher when they are closer to each other than when they are farther from each other. We assume that, for the same stress and injection conditions and the same distance between hypocenters, when the fault planes of two events are parallel and they are parallel to the line connecting hypocenters, the probability for these events to link is higher than this probability for other mutual orientations of fault planes. Moreover, when they have linked they more likely extend farther than the linked fractures with other fault plane orientations. We assume that linked fractures located along the straight line beginning at the injection point reach farther from this point than such fractures located in another way.

Consequently, seismic events are represented by eight parameters: three hypocentral coordinates, three independent angles determining orientations of the T and P axes of the double-couple focal mechanisms, and two angular coordinates of hypocenters in the spherical system beginning at the open hole of injection well. To achieve the same scaling of these parameters, we transform them to equivalent dimensions (ED) (Lasocki, 2014; Supporting Information Text S1). The average distance between the events in the 8-dimensional space of the aforementioned parameters, called the degree of disordering of sources, ZZ , expresses to which extent the above three conditions have been fulfilled. The chance for the seismic events with small value of ZZ , that they link and reach far is higher than in other cases. In this way ZZ quantifies the potential for building far-reaching fluid migration pathways.

We show that ZZ is highly significantly correlated with injection rate. ZZ took the highest values when the injection rates were the highest, which indicates that high injection rates counteracted the formation of far-reaching fluid migration pathways.

2 Data and Methods

The Geysers geothermal field is located in California, US. Geothermal operations, which began there in 1960s, and which presently use EGS technology, have induced hundreds of thousands of seismic events. We studied injection and seismic data from an isolated area of 2 km \times 2 km in the NW part of The Geysers, between 10 December 2007 and 23 August 2014. The basis for the seismic dataset was an improved catalog that contained 1252 events (Kwiatk et al., 2015; Martínez-Garzón et al., 2014; 2016). This catalog provided all the event parameters, necessary for the calculation of the degree of disordering of sources, ZZ : hypocenter locations with an accuracy of 50 m, and focal mechanisms with an accuracy of 20°/5°/10° for strike/dip/rake. The focal mechanisms were used to recover the trend and plunge angles of T and P axes. Moment magnitude was used and the completeness level was $M_c=1.4$ (Kwiatk et al.,

2015). The strongest event was Mw3.2. Hypocenter locations and magnitude distributions are provided in Supporting Information Figures S1-S5.

In the study period, the injections in the study area were carried out into two wells: Prati9 and Prati29. There were three phases of the injection activity:

- Phase F1 from 10 December 2007 to 10 April 2010, in which only Prati9 was operational,
- Phase F2 from 11 April 2010 to 21 June 2013 with simultaneous injections into both wells,
- Phase F3 from 11 June 2013 to the end of the study period, in which only Prati9 was operational.

The injection data consisted of the daily injection volumes into Prati9 and Prati29.

Most of the 1252 seismic events clustered around the open hole of Prati9 well (see: Supporting Information Figures S1-S4). We intended to analyze the relationship between injection and the degree of disordering of sources, ZZ , within the whole time period of available data, in which period only Prati9 well was constantly operational. Therefore we studied these events located closer to Prati9 well, expecting that their spatial relation to Prati9 resulted from their physical relation to the injection activity in Prati9. As the selection criterion we used the hypocentral distance from the open hole of Prati9 to be no more than 600 m. 1121 events that fulfilled this criterion are called cluster A.

The degree of disordering of sources, ZZ , used to quantify the potential for building the far-reaching fluid migration pathways, was the average distance between the seismic events in the 8-dimensional parameter space $\{x_1, x_2, x_3, plu_X_1, plu_X_2, tre_X_1, \Theta, \varphi\}$. $x_{1,2,3}$ were hypocenter coordinates. plu_X_1, tre_X_1 were the plunge and trend angles of T axis. plu_X_2 was the plunge angle of P axis. Θ, φ were the polar and azimuthal angles of hypocenter in the spherical system of coordinates beginning at the open hole of Prati9 well. $\Theta=0$ for the vertical direction and $\varphi=0$ for the N direction. These parameters were not comparable therefore we first transformed them to ED. The transformation to ED is a technique based on a probabilistic equivalence of the parameters that scale differently (Lasocki, 2014; Supporting Information Text S1). All transformed parameters are uniformly distributed in [0,1] and the distance between any two objects is the Euclidean metric. Further on the symbols $x_1, x_2, x_3, tre_X_1, tre_X_2, plu_X_1, plu_X_2, \Theta, \varphi$ denote the EDs of the original source parameters.

The closeness of hypocenters was parameterized by the absolute differences between hypocenter coordinates, $\Delta x_k(i, j) = |x_k(i) - x_k(j)|, k = 1, 2, 3$.

The trend angle and the polar angle take values in $[0^\circ, 180^\circ]$, which is $[0, 1]$ in ED, and the azimuthal angle takes values in $[0^\circ, 360^\circ]$, which is also $[0, 1]$ in ED. The shortest distances between these angles in ED were therefore:

$$\Delta tre_X_1(i, j) = 2 \begin{cases} |tre_X_1(i) - tre_X_1(j)| & \text{if } |tre_X_1(i) - tre_X_1(j)| \leq 0.5 \\ 1 - |tre_X_1(i) - tre_X_1(j)| & \text{if } |tre_X_1(i) - tre_X_1(j)| > 0.5 \end{cases} \quad (1)$$

$$\Delta \theta(i, j) = 2 \begin{cases} |\theta_i - \theta_j| & \text{if } |\theta_i - \theta_j| \leq 0.5 \\ 1 - |\theta_i - \theta_j| & \text{if } |\theta_i - \theta_j| > 0.5 \end{cases} \quad (2)$$

$$\Delta\varphi(i, j) = 4 \begin{cases} |\varphi(i) - \varphi(j)| & \text{if } |\varphi(i) - \varphi(j)| \leq 0.25 \\ |0.5 - |\varphi(i) - \varphi(j)|| & \text{if } 0.25 < |\varphi(i) - \varphi(j)| \leq 0.75 \\ 1 - |\varphi(i) - \varphi(j)| & \text{if } |\varphi(i) - \varphi(j)| > 0.75 \end{cases} \quad (3)$$

The multipliers in front of the opening braces in equations (1-3) were inserted so that the differences in all parameters scaled in [0, 1].

The plunge angle takes values in $[0^\circ, 90^\circ]$, hence, $\Delta plu_X_k(i, j)$ was always $|plu_X_k(i) - plu_X_k(j)|$, $k=1,2$.

For a collection of n seismic sources the degree of disordering of sources, ZZ reads:

$$ZZ = \left\{ \sum_{i=1}^{n-1} \sum_{j=i+1}^n ZZ(i, j) \right\} / \frac{n(n-1)}{2} \quad (4)$$

where

$$ZZ(i, j) = \frac{\sqrt{[\sum_{k=1}^3 \Delta x_k(i, j)^2] + [\Delta tre_X_1(i, j)^2 + \sum_{k=1}^2 \Delta plu_X_k(i, j)^2] + [\Delta \theta(i, j)^2 + \Delta \varphi(i, j)^2]}}{\sqrt{\Delta_r(i, j)^2 + \Delta_M(i, j)^2 + \Delta_\phi(i, j)^2}} \quad (4a)$$

$\Delta_r(i, j)$ is the distance between hypocenters of events i and j ;

$\Delta_M(i, j)$ is the distance between focal mechanisms of these two events;

$\Delta_\phi(i, j)$ is the distance between the directions of radii from the Prati9 open hole, those on which the hypocenters of these two events locate.

We carried out our analyses separately in the three injections phases. Out of 1121 studied events, 248 events occurred in the injection phase F1, 702 events – in phase F2 and 171 events – in phase F3. For every injection phase we calculated ZZ for 50-event window sliding by 10 events because the number of events per phase was not high enough to use non-overlapping windows. We obtained 21 ZZ values for F1, 66 ZZ values for F2 and 13 ZZ values for F3.

Next, we calculated the average injection rates, IN , during time windows covering the periods of the 50-event sliding windows, respectively. The calculations were performed for the injection rate periods exactly matching the periods of respective 50-event windows and for the injection rate periods from 1 to 21 days preceding the periods of event windows. The latter part of this analysis was meant to study delayed reactions of seismicity.

Finally, we studied the correlation between ZZ and IN . It comes from equation (4a) that ZZ is composed of three components representing our three conditions determining the potential of injection-induced seismicity for building far-reaching pathways for fluid migration. In order to recognize contributions of these components to the correlations between ZZ and IN we studied also the correlations between Δ_r , Δ_M , Δ_ϕ and IN , respectively.

All correlation analyses were preceded by the Jarque-Bera test applied to check normality of the distributions of used variables. If the normality hypothesis was not rejected we used Pearson correlation, otherwise we used Spearman correlation.

We also tested differences between the values of location parameters by phase of IN , ZZ , seismic activity rate and magnitude, respectively. When the normality hypothesis for a parameter

was not rejected, we used the Student's t-test for means, otherwise we applied the Mann-Whitney U-test for medians. All statistical inferences were performed under the significance level $\alpha=0.05$.

3 Results and Discussion

Some descriptive statistics by injection phase of *IN*, *ZZ*, seismic activity rate and magnitude of events are presented in Table 1 together with comparisons of their location parameters (means or medians) among phases. The medians of injection rates into Prati9 well were decreasing statistically significantly with injection phase.

Figure 1 compares the time-variations of *ZZ*, with the variations of average injection rate, *IN*. In phase F2 this comparison concerns the injection rate into Prati9 well, *IN*(9), and the total injection rate into both wells, *IN*(both). It is seen that in the first two injection phases, F1 and F2, *ZZ* correlated positively with *IN*. Also the amplitudes of the *ZZ*-changes agreed well with the amplitudes of the average injection rate changes. In phase F2, this agreement related to the summed injection into both wells (blue curve) rather than into Prati9 well alone (black curve), even though the analyzed seismic events were geometrically linked to Prati9 (Supporting Information Figures S1-S4).

Table 2 presents the results of analysis of correlations between the injection rate, *IN*, and *ZZ*. For all average injection rate series and for most *ZZ* and its components' series the normality hypothesis was not rejected. For these cases the analysis was based on Pearson's linear correlation coefficient. The exceptional cases were correlations with $\Delta\phi$ in phase F2 because $\Delta\phi$ series in this phase was not normally distributed. In these two cases Spearman's rank correlation was used.

The results in Table 2 confirm the relationships evidenced in Figure 1. In F1 and F2 the correlation between *IN* and *ZZ* was significant, positive. In F2 this correlation was highly significant, irrespective of whether the *IN* referred to injections into Prati9 or to the summed injections into Prati9 and Prati29 wells. The *ZZ* vs. *IN*(9) scatterplot is presented in Supporting Information Figure S6.

The results of correlation analysis for delayed *ZZ* with respect to *IN* are presented in Supporting Information Tables S1-S4. In F1 the correlation coefficient slowly decreases with increasing lag. The correlation coefficient in F2 slightly increased when *ZZ* was delayed with respect to *IN*, however the difference between the correlation coefficient for zero lag and for 13 days lag was only 0.022 and was surely insignificant.

The previous studies of the same data have indicated a positive correlation between seismicity rates and injection rates (Leptokaropoulos et al., 2018). Hence different time periods corresponded here to the 50-events windows; the time periods at higher injection rates were shorter. We checked whether the positive *ZZ* vs. *IN* correlations were not due to these differences between time periods. We divided phase F2 into non-overlapping windows of constant, 68 days duration. The correlation between *IN* and *ZZ* both calculated for these windows of constant time period, was also positive (0.87) and significant ($p = 0.0097$).

In F1 only Δ_r out of three components of ZZ significantly and positively correlated with *IN*. Hence, in this injection phase the positive ZZ - *IN* correlation resulted from that that higher injection rates were increasing distances between the sources.

In F2 all three distances, Δ_r , Δ_M , Δ_ϕ , were highly positively correlated with *IN* thus they all significantly contributed to the correlation ZZ – *IN*. Higher injection rates led to an increase of the distances between hypocenters, to a greater variety of P and T axes directions and to a greater angular dispersion of the hypocenters in relation to the open hole of Prati9 well.

The significant correlation Δ_r – *IN* in F1 and F2 cannot be attributed just to moving away sources from the well opening of Prati9 when the injection rates were higher. The correlation between the average distance from the Prati9 opening and *IN* was significant in F1 (corr. coefficient 0.47, $p=0.03$), though much weaker than the Δ_r – *IN* correlation, and in F2 it was insignificant (corr. coefficient 0.14, $p=0.28$).

Our target was studying the relationship between the degree of disordering of seismic sources, ZZ, and the injection rate, *IN*. We used the transformation to ED because the components of ZZ: the distances between *P* (and *T*) axes of events and the distances between radii on which events located, are not Euclidean. However, the metrics of the distance between hypocenter locations is Euclidean. Thus, it was possible to compare the shown here results of correlation between Δ_r and *IN* in F1 and F2, based on the transformation to ED, with such results based on more often used inter-event distance analyses. As alternatives to Δ_r we used correlation dimension of distances between hypocenters, D_2 , and summarized squared distances in the original (*x,y,z*) space, $d2$. D_2 turned out to be uncorrelated with *IN*, probably because difficulties with its estimation. The correlation between $d2$ and *IN* was even stronger than between Δ_r and *IN*. We think that this was due to the fact that any transformation, here the transformation to ED causes some loss of information. Nevertheless, the same significant correlation between $d2$ and *IN* as the correlation between Δ_r and *IN* positively validated the performance of transformation to ED. The results of this part of analysis are provided and discussed in Supporting Information Text S2.

The significant impact of fluids on the stress field and the faulting regime is known from many studies (e.g., Segall and Fitzgerald, 1998; Hardebeck and Hauksson, 1999; Bachmann et al., 2012). The analyses of seismic events from the NW part of The Geysers geothermal field, presented in Martínez-Garzón et al. (2013, 2016) and Kwiątek et al. (2015), clearly show a large variability of focal mechanisms. Explaining the observed stress tensor perturbation the cited authors consider the fact that in addition to fracture reactivation, massive fluid injection in EGS systems results in hydro-fracturing. It is then possible that during the time periods of higher injection rates, new small fractures were created and they could also perturb the stress field in the observed way (Martínez-Garzón et al., 2016). A number of events occurred either on severely misoriented faults (low instability coefficient, eg. Vavryčuk, 2011) or slipped in a different orientation than the predicted from the stress field. These events mostly occurred during periods of high injection rates indicating that faults not optimally oriented to the stress field require larger pore pressures to become activated.

A way in which increased injection rates may increase the degree of disordering of sources (ZZ) is shown schematically in Figure 2. An increase of pore pressure resulting from the increased injection rate broadens the range of possible orientations and locations for new shear fractures.

Studying fracture network development on the same data as here, Orlecka-Sikora et al. (2019) have shown that the connectivity of fractures induced by fluid injection is lower for higher injection rates and *vice versa*. Thus the connectivity was responding to the injection rate changes in the same way as ZZ . This allows for inferring that ZZ indeed represents the potential for fluid migration. In the cited work the connectivity was estimated by the connectivity coefficient, C , defined by the ratio of the observed number of intersections of fractures in a fracture network to the number of all possible intersections in this network. These all possible intersections were evaluated as $0.5f(f - 1)$, where f was the number of fractures building the fracture network (Albert & Barabasi, 2002; Watts & Strogatz, 1998).

Prati29 well was operational only in phase F2. In this phase the amplitudes of ZZ changes agreed with the amplitudes of changes of the summarized injections into Prati9 and Prati29. Furthermore, the mean level of ZZ and the mean seismic activity were the highest in this phase and significantly higher than in phases F1 and F3. In F2 only the level of total injection into Prati9 and Prati29 was the highest, and the mean level of injection rate into the Prati9 well was significantly smaller than in phase F1. All these indicate the important role of the injections into Prati29 for the generation of seismic events within the studied cluster A despite the Prati29 well location being outside cluster A.

The seismic events generated at higher injection rates, i.e. the ones more disordered (ZZ was higher), did not have greater magnitudes. On the contrary, in phase F1 the mean magnitude in windows correlated negatively with ZZ (corr. coef. -0.61 , $p = 0.003$). In F2 no magnitude – ZZ correlation was ascertained.

In phase F3, in which the overall level of injection rate was the lowest among injection phases, the correlation $IN - ZZ$, was significant, negative. This correlation was achieved only jointly by the three components of ZZ : Δ_r , Δ_M , Δ_ϕ because neither of them significantly correlated with IN . The negative correlation coefficient in F3 increased when ZZ was delayed with respect to IN , and for 4 and more days lag it became statistically not significant (Supporting Information Table S4). This reversal of correlation results may be connected with another fracture mechanism below a certain level of injection rate. We discuss this possibility in Supporting Information Text S3. However, the data series in F3 was composed of only 13 points therefore the correlation ($p \approx 0.03$) might be spurious.

4 Conclusions

Studying the actual field data we found exceptionally high and immediate correlation between the injection rate and the seismicity parameter - the degree of disordering of sources, ZZ . Also the amplitudes of ZZ -changes agreed well with the amplitudes of average injection rate changes. ZZ is defined solely on parameters of seismic sources. It describes how much seismic fractures are dispersed in terms of distances between their hypocenters, mutual orientations of their fracture planes, and angular dispersion of their hypocenters. In the next work we will modify ZZ to account also for source sizes.

We interpret ZZ as a measure of the potential of seismic fractures for building far-reaching pathways for fluid migration. The logic of the three conditions, on which ZZ is based, supports this interpretation. However, ZZ does not represent all possibilities for building such a fracture system neither it is adequate for other possibilities of fracture network development (e.g. not for a percolating fluid pathway).

In the studied case from The Geysers geothermal field, the optimal conditions to avoid such ordering of seismic fractures that enable linking them into longer pathways, extending farther from the injection point were met for high injection rates. The higher the injection rate was, the more disordered the seismic fractures were generated, i.e., the chances to build longer pathways for undesired fluid migration decreased. High injection rates caused an increase in seismic activity, nevertheless the median level of seismic event magnitudes remained unaffected.

The above conclusion, if confirmed in other cases of injection induced seismicity, would help to understand this type of seismicity and related hazards. Martínez-Garzón, et al. (2018) conclude that the used here dataset from the NW region of The Geysers well represents the broader seismic processes at The Geysers field. Thus our results may be also valid for all seismic processes at The Geysers. However, for further generalizations studies of other injection-induced seismicity cases are required.

Acknowledgments

We thank the Calpine Corporation for providing high-resolution hydraulic data from The Geysers field. The comments and suggestions of two anonymous Reviewers were much appreciated. This work was supported under the S4CE: "Science for Clear Energy" project, which has received funding from the European Union's Horizon 2020 research and innovation programme, under grant agreement No 764810. The work was also partially supported by statutory activities No 3841/E-41/S/2018 of the Ministry of Science and Higher Education of Poland. Data are available on the IS-EPOS platform of Thematic Core Service Anthropogenic Hazards (https://tcs.ah-epos.eu/#episode:THE_GEYSERS_Prati_9_and_Prati_29_cluster, doi: 10.25171/InstGeoph_PAS_ISEPOS-2017-011).

References:

- Albert, R. & Barabasi, A.L. (2002) Statistical mechanics of complex network, *Reviews of Modern Physics*, 74, 47–97.
- Bachmann, C.E., Wiemer, S., Goertz-Allmann, B.P. & Woessner, J. (2012) Influence of pore-pressure on the event-size distribution of induced earthquakes, *Geophysical Research Letters*, 39, L09302, doi:10.1029/2012GL051480
- Chorozoglou, D., Kugiumtzis, D., & Papadimitriou, E. (2018) Testing the structure of earthquake networks from multivariate time series of successive main shocks in Greece, *Physica A*, 499, 28–39.
- Davies, R., Foulger, G., Bindley, A., & Styles, P. (2013) Induced seismicity and hydraulic fracturing for the recovery of hydrocarbons, *Marine and Petroleum Geology*, 45, 171–185.
- Ellsworth, W.L. (2013) Injection-induced earthquakes, *Science*, 341, 6142, doi: 10.1126/science.1225942
- Hardebeck, J.L. & Hauksson, E. (1999) Role of fluids in faulting inferred from stress field signatures. *Science* 285 (5425), 236–239, DOI: 10.1126/science.285.5425.236
- Hope, S.M., Davy, P., Maillot, J., Le Goc, R., & Hansen, A. (2015) Topological impact of constrained fracture growth. *Frontiers in Physics* 3–75.
- Kagan, Y.Y. (1992) Correlations of earthquake focal mechanisms. *Geophysical Journal International*, 110, 305–320.
- Kagan, Y.Y. (2000) Temporal correlations of earthquake focal mechanisms. *Geophysical Journal International*, 143, 881–897.
- Ko, T.Y., & Kemeny, J. (2011) Subcritical crack growth in rocks under shear loading. *Journal of Geophysical Research, Solid Earth*, 116, B01407, doi:10.1029/2010JB0008461.
- Kwiatek, G., Martínez-Garzón, P., Dresen, G., Bohnhoff, M., Sone, H., & Hartline, C. (2015) Effects of long-term fluid injection on induced seismicity parameters and maximum magnitude in northwestern part of The Geysers geothermal field. *Journal of Geophysical Research, Solid Earth*, 120, 7085–7101, doi: 10.1002/2015JB012362.
- Lasocki, S. (2014) Transformation to equivalent dimensions – a new methodology to study earthquake clustering. *Geophysical Journal International*, 197 (2), 1224–1235.
- Lee, J.S., Veneziano, D., & Einstein, H.H. (1990) “Hierarchical fracture trace model” In *Rock Mechanics Contributions and Challenges: Proceedings of the 31st US Symposium on Rock Mechanics*, W. Hustrulid, W., & Johnson, G.A., Eds. (A.A. Balkema 1990), pp. 261–268.
- Leptokaropoulos, K., Staszek, M., Lasocki, S., Martínez-Garzón, P., & Kwiatek, G. (2018) Evolution of seismicity in relation to fluid injection in the North-Western part of The Geysers geothermal field. *Geophysical Journal International*, 212, 1157–1166, doi: 10.1093/gji/ggx481
- Lockner, D.A., Byerlee, J., Kuksenko, V., Ponomarev, A., & Sidorin, A. (1992) “Observations of quasi-static fault growth and acoustic emissions” in *Fault Mechanics and Transport Properties of Rocks*, B. Evans and T.-F. Wong, Eds. (Academic, London 1992), pp. 3–31.
- Long, J.C.S., & Billaus, D.M. (1987) From field data to fracture network modeling: An example incorporating special structure, *Water Resources Research*, 23(7), 1201–1216.
- Majer, E., Nelson, J., Robertson-Tait, A., Savy, J., & Wong, I. (2012) Protocol for Addressing Induced Seismicity Associated with Enhanced Geothermal Systems, *Geothermal Technologies Program U.S. Department of Energy, Energy Efficiency & Renewable Energy*
- Martínez-Garzón, P., Bohnhoff, M., Kwiatek, G. & Dresen, G. (2013) Stress tensor changes related to fluid injection at The Geysers geothermal field, California, *Geophysical Research Letters*, 40, 2596–2601, doi:10.1002/grl.50438

- Martínez-Garzón, P., Kwiatek, G., Sone, H., Bohnhoff, M., Dresen, G., & Hartline, C. (2014) Spatiotemporal changes, faulting regimes, and source parameters of induced seismicity: A case study from The Geysers geothermal field. *Journal of Geophysical Research. Solid Earth*, 119, 8378–8396, doi: 10.1002/2014JB011385.
- Martínez-Garzón, P., Kwiatek, G., Bohnhoff, M., & Dresen, G. (2016) Impact of fluid injection on fracture reactivation at The Geysers geothermal field, *Journal of Geophysical Research. Solid Earth*, 121(10), 7432–7449, doi: 10.1002/2016JB013137.
- Martínez-Garzón, P., Zaliapin, I., Ben-Zion, Y., Kwiatek, G. & Bohnhoff, M. (2018) Comparative study of earthquake clustering in relation to hydraulic activities at geothermal fields in California. *Journal of Geophysical Research. Solid Earth*, 123, 4041–4062, <https://doi.org/10.1029/2017JB014972>.
- Orlecka-Sikora, B., Cielesta, S., & Lasocki, S. (2019) Tracking the development of seismic fracture network from The Geysers geothermal field. *Acta Geophysica*, 67, 341–350.
- Sausse, J.C., Dezayes, C., Dorbath, L. Genter, A., & Place, J. (2010) 3D model of fracture zones at Soultz-sous-Forêts based on geological data, image logs, induced microseismicity and vertical seismic profiles. *Comptes Rendus Geo-sciences*, 342(7-8), 531–545.
- Schwartz, F.W., Smith, L. & Crowe, A.S. (1983) A stochastic analysis of macroscopic dispersion in fractured media, *Water Resources Research*, 19(5), 1253–1265.
- Segall, P. & Fitzgerald, S.D. (1998) A note on induced stress changes in hydrocarbon and geothermal reservoirs. *Tectonophysics*, 289, 117–128.
- Snow, D.T. (1965) A parallel plate model fractured permeable media, PhD. Thesis, Univ. of Calif., Berkeley.
- Stanchits, S., Dresen, G., & Guéguen, Y. (2006) Ultrasonic velocities, acoustic emission characteristics and crack damage of basalt and granite, *Pure Applied Geophysics*, 163(5–6), 975–994.
- Vavryčuk, V. (2011) Principal earthquakes: theory and observations from the 2008 West Bohemia swarm, *Earth and Planetary Science Letters*, 305, 290–296, doi: 10.1016/j.epsl.2011.03.002.
- Warren-Smith, E., Fry, B., Wallace, L., Chon, E., Henrys, S., Sheehan, A., Mochizuki, K., Schwartz, S., Webb, S. & Lebedev, S. (2019) Episodic stress and fluid pressure cycling in subducting oceanic crust during slow slip. *Nature Geoscience*, 12, 475–481, doi.org/10.1038/s41561-019-0367-x.
- Watts, D.J. & Strogatz, S.H. (1998) Collective dynamics of “small-world” networks, *Nature*, 393, 440–442.
- Zhang Dongxiao & Yang Tingyun (2015) Environmental impacts of hydraulic fracturing in shale gas development in the United States, *Petroleum Exploration and Development*, 42(6), 876–883.

Tables:

Table 1. Descriptive statistics and comparisons of the average injection rate, IN , the degree of disordering of seismic sources, ZZ , the activity rate, and magnitude of events in the three injection phases. The magnitude was transformed to the equivalent dimension. The other quantities: IN and activity rate were not. The column “Comparisons” contains p -values of the tests of differences between means or medians of these parameters. The significant differences are in bold.

	Injection phase									Comparisons of location parameters, p -value		
	F1			F2			F3			F1 vs. F2	F2 vs. F3	F1 vs. F3
	Mean	Med.	Std. dev.	Mean	Med.	Std. dev.	Mean	Med.	Std. dev.			
Prati9 IN [100m ³ /day]	43.76	45.18	13.09	36.18	35.69	11.51	29.10	30.95	8.18	0.024	0.014	3E-4
Summed Prati9 and Prati29 IN [100m ³ /day]	43.76	45.18	13.09	72.82	73.43	22.54	29.10	30.95	8.18	-----		
ZZ	1.402	1.403	0.012	1.439	1.438	0.021	1.401	1.396	0.015	5E-14	2E-7	0.91
Activity rate [event/day]	0.35	0.34	0.13	0.70	0.69	0.23	0.48	0.44	0.11	7E-12	6E-6	7E-3
Magnitude	0.55	0.57	0.06	0.49	0.49	0.04	0.45	0.47	0.06	3E-4	0.055	2E-4

Table 2. Results of the correlation analysis between the average injection rate, IN , and ZZ , and its components, Δ_r , Δ_M , Δ_ϕ . For phase F2 row ‘a’ provides the correlation between ZZ and IN into Prati9 well, and row ‘b’ provides the correlation between ZZ and total IN into Prati9 and Prati29 wells. The significant correlations are in bold. The results based on Spearman rank correlation are in italics.

Injection phase	ZZ		Δ_r		Δ_M		Δ_ϕ	
	Corr. coef.	p -value	Corr. coef.	p -value	Corr. coef.	p -value	Corr. coef.	p -value
F1	0.62	0.002	0.69	5·10⁻⁴	0.20	0.37	-0.28	0.22
F2 – a	0.76	2·10⁻¹³	0.69	2·10⁻¹⁰	0.41	7·10⁻⁴	0.49	3·10⁻⁵
F2 – b	0.72	7·10⁻¹²	0.65	1·10⁻⁹	0.45	1·10⁻⁴	0.47	8·10⁻⁵
F3	-0.60	0.029	-0.20	0.51	-0.32	0.28	-0.19	0.52

Figure captions:

Figure 1. Comparison of the time-variation of ZZ with the time-changes of average injection rate. Black – the injection rate into Prati9 well, blue – the total injection rate into Prati9 and Prati29 wells, brown – ZZ . The horizontal bars mark the durations of injection phases.

Figure 2. Schematic presentation of influence of pore pressure (P) changes on the failure plane orientations. The linear failure criterion imposes that shear fractures make with σ_1 a well-defined angle of $(\pm) 45^\circ - \phi/2$, where ϕ is the angle of internal friction, and $\theta = \phi/2 + 45$ (gray circle in Coulomb-Mohr diagram and gray fractures on the rock block on the left). An increase of P reduces the effective normal stress, σ_n' , where $\sigma_n' = \sigma_n - P$ and broadens the range of possible orientations for new shear fractures (all directions going through green hatched area in the Coulomb-Mohr diagram and green fractures on the rock block) (after Warren-Smith et al., 2019).

**High injection rates counteract formation of far-reaching fluid migration pathways at
The Geysers geothermal field**

Stanisław Lasocki¹, and Beata Orlecka-Sikora¹

¹Institute of Geophysics Polish Academy of Sciences

Contents of this file

Text S1 Summary of the transformation to equivalent dimension technique.
Figures S1 – S5 Hypocenter locations and magnitude distributions.
Figure S6 Scatterplot of the degree of disordering of sources, ZZ, vs. average injection rate into Prati9 well, $IN(9)$.
Tables S1 – S4 Results of the analysis of correlation between for the average injection rate, $IN(9)$ and the degree of disordering of sources, ZZ for different lag time between $IN(9)$ and ZZ.
Text S2 Comparison of the results of correlation analysis for different representations of closeness of hypocenters.
Text S3 Discussion of the results of correlation analysis for phase F3 of injection.

Introduction

Text S1 presents briefly the transformation to equivalent dimension technique. This transformation was applied to eight parameters that represented seismic events in calculations of the degree of disordering of sources, ZZ. ZZ was determined by distances between the events seen as points in 8D space of these parameters. ZZ could not be evaluated from original values of these parameters because these parameters were not comparable and five of them did not have the Euclidean metric. The transformation to equivalent dimensions is suited for such problems. After transformation any set of parameters becomes comparable and the parameter space metric becomes Euclidean. The text S1 presents the problem, provides the assumptions of the transformation, defines equivalent dimensions, presents their

properties and the algorithm of the transformation. The address of the web page from where the MATLAB codes of the transformation can be downloaded is also provided.

Figures S1 to S4 present the locations of hypocenters of the analyzed seismic events in the 3D view and in the three 2D projections. The events marked by blue circles indicate locations of the event from the cluster A, which have been analyzed in this paper. The other events from the initial dataset are marked by black squares. The size of markers is proportional to the magnitude of events. Locations of the open holes of the injection wells Prati9 and Prati29 are also provided.

Figures S5 presents magnitude distribution of all events as well as of the events from particular injection phases.

Figure S6 presents the scatterplots of the degree of disordering of sources, ZZ vs. the average injection rate into Prati9 well, $IN(9)$, in the injection phases F1 and F2.

Tables S1-S4 complement Table 2 and present the results of the correlation analysis between the injection rate, IN , and the degree of disordering of sources, ZZ and the three components of ZZ for the ZZ and its components delayed with respect to IN values from zero to 21 days, step one day. Table S1 contains the results for the injection phase F1, Tables S2 and S3 contain the results for the injection phase F2 and Table S4 contains the results for the injection phase F3. The results in Table S2 relate to the correlations with the injections into the injection well Prati9 and the results in Table S3 relate to the correlations with the summed injections into Prati9 and Prati29 wells.

Text S2 compares the results of correlation analysis between injection rate and three different representations of closeness of hypocenters namely: (1) the average distance between hypocenters in equivalent dimension space, Δ_r – the parameter used in the main text, (2) the correlation dimension of distance between hypocenters, (3) the summarized squared distance between hypocenters in original Cartesian system of coordinates. The comparison has been performed on the data from phase F1.

In Text S3 we present a possible explanation of the obtained in phase F3 anticorrelation between the degree of disordering of sources, ZZ , and the injection rate.

Text S1. Summary of the transformation to equivalent dimension technique (Lasocki, 2014)

Parameters of Seismic Events

- Source parameters: $t, lat, lon, depth, M, [M_{ij}], E_s, \Delta\sigma, r_0$ etc.
- Derived from source parameters of two or more events e.g.: interevent time - τ , distance between this and the main shock - r , etc.
- Other having unambiguous association with seismic events e.g.
 - Parameters of the environment in which the event occurs: e_1, e_2, e_3
 - Parameters of inducing technological activity for anthropogenic seismicity: $l_1, l_2, l_3 \dots$
 -

A seismic event \equiv A point in a parameter space e.g. : $\mathbf{X} = [t, lat, lon, depth, M, [M_{ij}], E_s, \Delta\sigma, r_0, \dots, \tau, r, \dots, e_1, e_2, e_3, \dots, l_1, l_2, l_3, \dots, \dots]$

Problem: Parameters of seismic events are not comparable and may have non-Euclidean metric.

Equivalent dimensions – Assumptions:

- Let seismic events be represented by the set of parameters $X_k, k=1, \dots, p$. The population of these events is fully characterized by the probabilistic distributions of the parameters $F(X_k), k=1, \dots, p$.
- Two intervals of the parameter values, $[x_{k,i}, x_{k,j}]$, $[x_{1,s}, x_{1,t}]$ are equivalent if $\text{Prob}(X_k \in [x_{k,i}, x_{k,j}]) = \text{Prob}(X_1 \in [x_{1,s}, x_{1,t}])$.
- The parameters $X_k, k=1, \dots, p$, are continues random variables.

Equivalent dimension – Definition: The equivalent dimension of X is $U=F(X)$, where $F(X)$ is the cumulative distribution of X

Properties

- Every U is uniformly distributed in $[0,1]$
- $\{U_{i=1, \dots, p}\}$ has Euclidean metric
- The distance between the two seismic events, i, j , is

$$d(i, j) = \sqrt{\sum_{k=1}^p [U_k(i) - U_k(j)]^2}$$

Technique

- The probabilistic models for earthquake parameters, $F(X_k)$, are in general not known.
- If the earthquakes' data are a representative sample of size n , replace $F(X_k)$, $k=1,...,p$ with their data-driven, kernel estimators (Silverman, 1986):

$$\hat{F}_X(x|\{x_i, n\}) = \frac{1}{n} \sum_{i=1}^n \Phi\left(\frac{x - x_i}{\lambda_i h}\right)$$

where: $\Phi(u)$ is the cumulative distribution function of the standard normal distribution

h is the common smoothing factor e.g. the solution of the equation (Kijko, et al., 2001):

$$\sum_{i,j} \left\{ 2^{-0.5} \left[\frac{(x_i - x_j)^2}{2h^2} - 1 \right] \exp \left[-\frac{(x_i - x_j)^2}{4h^2} \right] - 2 \left[\frac{(x_i - x_j)^2}{h^2} - 1 \right] \exp \left[-\frac{(x_i - x_j)^2}{2h^2} \right] \right\} = 2n$$

λ_i are the local bandwidth factors e.g.: (Orlecka-Sikora & Lasocki, 2005)

$$\lambda_i = \left[\frac{\hat{f}^*(x_i|\{x_j, n\})}{g} \right]^{-0.5}$$

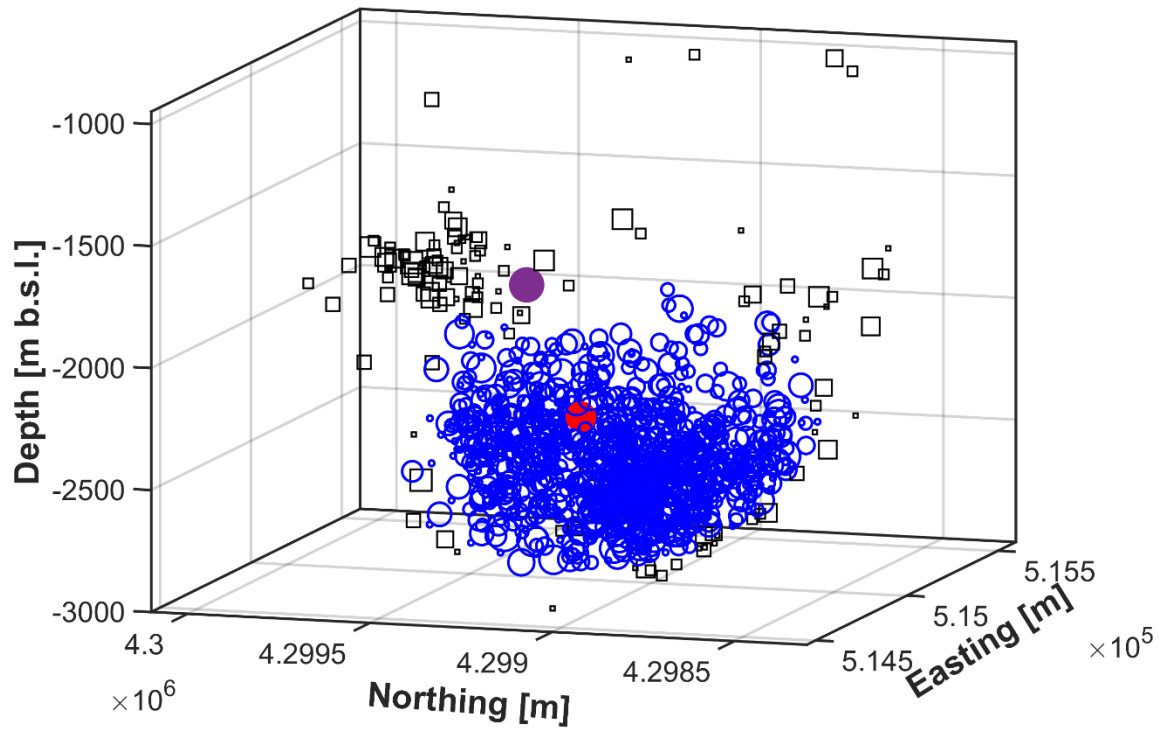
$$\hat{f}^*(x_i|\{x_j, n\}) = \frac{1}{\sqrt{2\pi}hn} \sum_{j=1}^n \exp \left[-\frac{(x_i - x_j)^2}{2h^2} \right] \quad g = [\prod_{i=1}^n \hat{f}^*(x_i|\{x_j, n\})]^{\frac{1}{n}}$$

The MATLAB toolbox with codes for equivalent dimension transformation can be downloaded from <https://git.plgrid.pl/projects/EA/repos/sera-applications/browse>

References:

- Kijko, A., Lasocki S., & Graham G. (2001) Nonparametric seismic hazard analysis in mines. *Pure and Applied Geophysics*, 158, 1655-1676.
- Lasocki, S. (2014) Transformation to equivalent dimensions – a new methodology to study earthquake clustering. *Geophysical Journal International*, 197 (2), 1224-1235.
- Orlecka-Sikora, B. & Lasocki, S. (2005) “Nonparametric characterization of mining induced seismic sources.” In: Proceedings Sixth International Symposium on Rockburst and Seismicity in Mines 9-11 March 2005, Australia, Potvin, Y., & Hudyma, M., Eds. (Australian Centre for Geomechanics, Nedlands 2005), pp. 555-560.
- Silverman, B.W. (1986) “Density Estimation for Statistics and Data Analysis” (Chapman and Hall, London, 1986).

127
128
129
130



131

132 **Figure S1.** 3D view of spatial distribution of hypocenters of 1252 events from the seismic catalog from
133 the NW region of The Geysers geothermal field. Blue circles indicate locations of the events from the
134 cluster A, which have been analyzed in this paper. The other events from the initial dataset are marked by
135 black squares. The size of markers is proportional to the magnitude of events. Big red dot marks the
136 position of the open hole section of the Prati9 well and big violet dot marks the position of the open hole
137 section of the Prati29 wells. The distances between the holes are: vertical – 386.8 m, horizontal – 479.5 m.
138

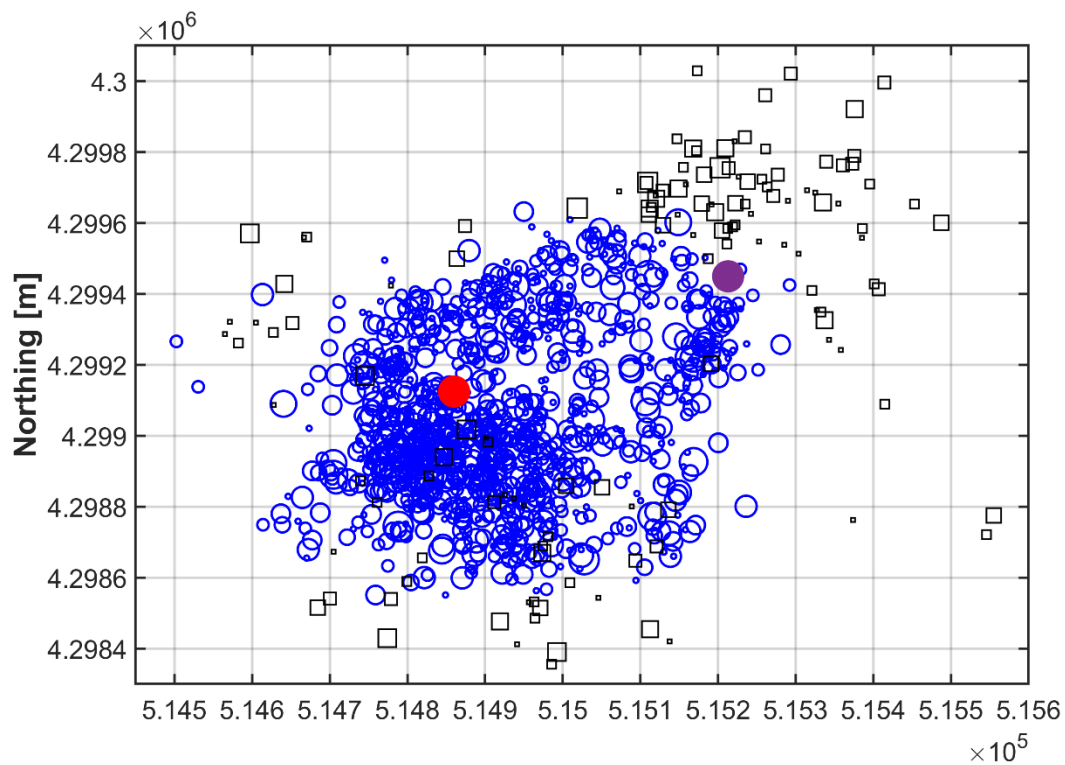


Figure S2. Horizontal projection of Figure S1.

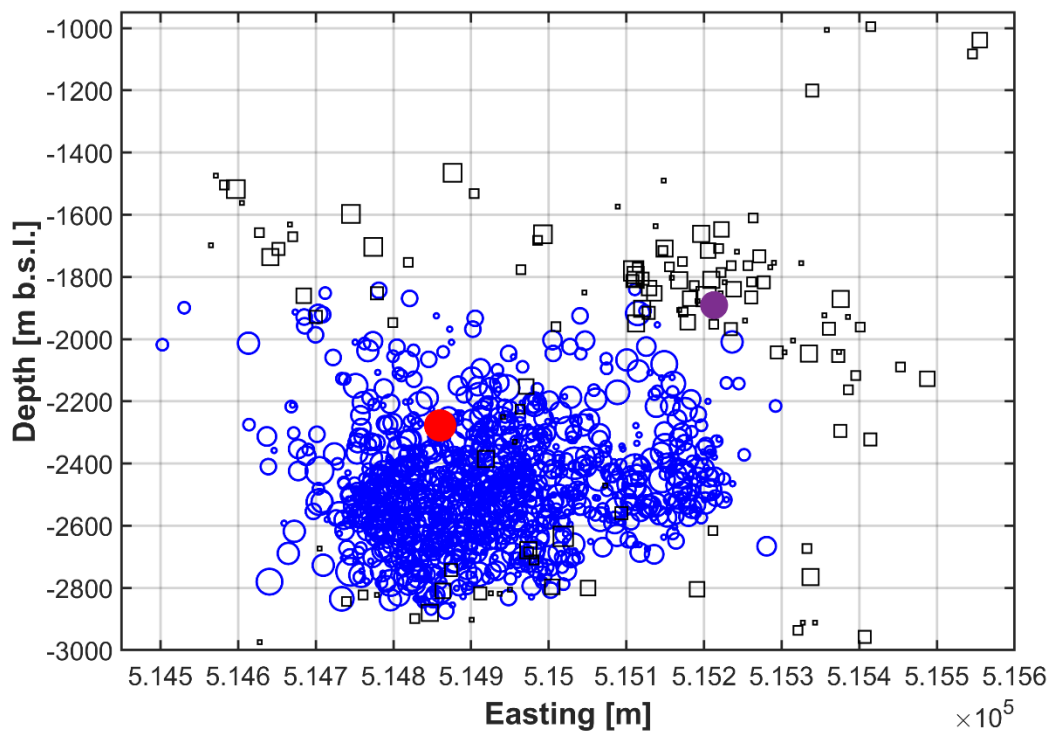


Figure S3. Vertical xz projection of Figure S2.

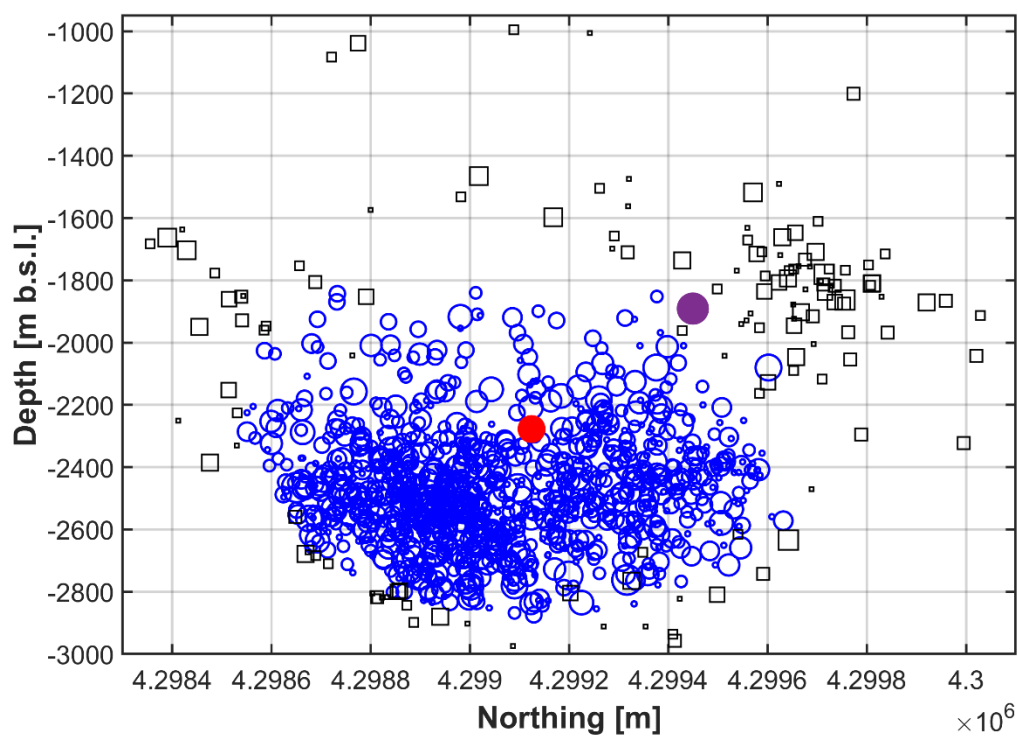


Figure S4. Vertical yz projection of Figure S2.

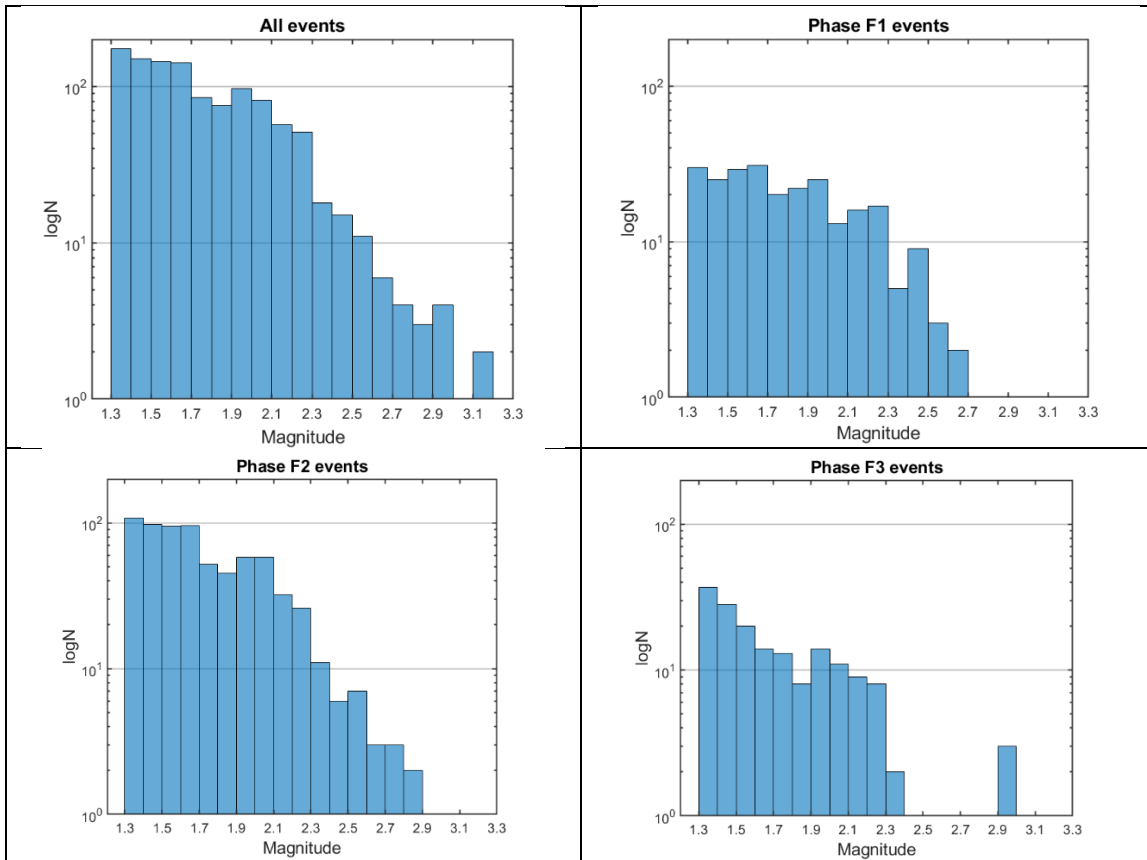


Figure S5. Magnitude-frequency histograms of studied events

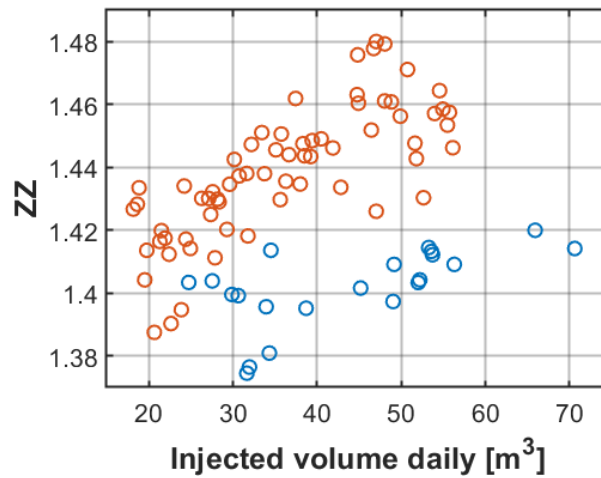


Figure S6. The degree of disordering of sources, ZZ vs. the average injection rate into Prati9 well, $IN(9)$ scatterplots. Blue markers – the scatterplot for the injection phase F1. Brown markers – the scatterplot for the injection phase F2.

Table S1. Results of the correlation analysis between the average injection rate, IN , and the degree of disordering of seismic sources, ZZ , and its components, Δ_r , Δ_M , Δ_ϕ for the phase F1. The correlation have been evaluated for ZZ , Δ_r , Δ_M , Δ_ϕ delayed from 0 to 21 days with respect to IN .

Delay [days]	ZZ		Δ_r		Δ_M		Δ_ϕ	
	Corr. coef.	p-value	Corr. coef.	p-value	Corr. coef.	p-value	Corr. coef.	p-value
0	0.623	2.5E-03	0.694	4.9E-04	0.205	3.7E-01	-0.280	2.2E-01
1	0.621	2.7E-03	0.688	5.7E-04	0.210	3.6E-01	-0.275	2.3E-01
2	0.618	2.9E-03	0.682	6.6E-04	0.214	3.5E-01	-0.270	2.4E-01
3	0.614	3.0E-03	0.676	7.8E-04	0.219	3.4E-01	-0.265	2.5E-01
4	0.611	3.3E-03	0.669	9.1E-04	0.223	3.3E-01	-0.260	2.6E-01
5	0.607	3.5E-03	0.662	1.1E-03	0.227	3.2E-01	-0.255	2.6E-01
6	0.603	3.8E-03	0.654	1.3E-03	0.231	3.1E-01	-0.248	2.8E-01
7	0.599	4.1E-03	0.648	1.5E-03	0.235	3.1E-01	-0.244	2.9E-01
8	0.594	4.5E-03	0.641	1.7E-03	0.239	3.0E-01	-0.240	2.9E-01
9	0.590	4.9E-03	0.634	2.0E-03	0.243	2.9E-01	-0.236	3.0E-01
10	0.586	5.3E-03	0.627	2.3E-03	0.247	2.8E-01	-0.233	3.1E-01
11	0.581	5.7E-03	0.621	2.7E-03	0.250	2.7E-01	-0.229	3.2E-01
12	0.577	6.2E-03	0.614	3.1E-03	0.254	2.7E-01	-0.226	3.2E-01
13	0.572	6.7E-03	0.607	3.5E-03	0.257	2.6E-01	-0.223	3.3E-01
14	0.568	7.2E-03	0.602	3.9E-03	0.263	2.5E-01	-0.223	3.3E-01
15	0.563	7.8E-03	0.595	4.4E-03	0.266	2.4E-01	-0.220	3.4E-01
16	0.559	8.4E-03	0.588	5.0E-03	0.270	2.4E-01	-0.216	3.5E-01
17	0.554	9.1E-03	0.581	5.7E-03	0.274	2.3E-01	-0.213	3.5E-01
18	0.550	9.8E-03	0.574	6.5E-03	0.279	2.2E-01	-0.209	3.6E-01
19	0.545	1.1E-02	0.567	7.4E-03	0.283	2.1E-01	-0.206	3.7E-01
20	0.542	1.1E-02	0.560	8.2E-03	0.288	2.1E-01	-0.201	3.8E-01
21	0.538	1.2E-02	0.553	9.3E-03	0.292	2.0E-01	-0.198	3.9E-01

Table S2. Results of the correlation analysis between the average injection rate into Prati9 well, $IN(9)$, and the degree of disordering of seismic sources, ZZ , and its components, $\Delta_r, \Delta_M, \Delta_\phi$ for the phase F2. The correlation have been evaluated for $ZZ, \Delta_r, \Delta_M, \Delta_\phi$ delayed from 0 to 21 days with respect to $IN(9)$. The results based on Spearman rank correlation are in italics.

Delay [days]	ZZ		Δ_r		Δ_M		Δ_ϕ	
	Corr. coef.	p-value	Corr. coef.	p-value	Corr. coef.	p-value	Corr. coef.	p-value
0	0.756	2.2E-13	0.687	1.9E-10	0.408	6.7E-04	<i>0.493</i>	<i>3.4E-05</i>
1	0.759	1.5E-13	0.693	1.1E-10	0.409	6.6E-04	<i>0.488</i>	<i>4.1E-05</i>
2	0.761	1.2E-13	0.698	7.6E-11	0.409	6.5E-04	<i>0.482</i>	<i>5.1E-05</i>
3	0.762	1.1E-13	0.701	5.8E-11	0.407	6.9E-04	<i>0.481</i>	<i>5.4E-05</i>
4	0.762	1.1E-13	0.703	4.5E-11	0.407	7.1E-04	<i>0.481</i>	<i>5.3E-05</i>
5	0.764	9.0E-14	0.707	3.1E-11	0.407	7.0E-04	<i>0.478</i>	<i>6.1E-05</i>
6	0.765	7.4E-14	0.711	2.1E-11	0.407	6.8E-04	<i>0.475</i>	<i>6.9E-05</i>
7	0.767	6.0E-14	0.715	1.5E-11	0.408	6.7E-04	<i>0.472</i>	<i>7.6E-05</i>
8	0.768	5.0E-14	0.719	1.0E-11	0.408	6.7E-04	<i>0.467</i>	<i>9.3E-05</i>
9	0.770	4.2E-14	0.723	7.0E-12	0.408	6.8E-04	<i>0.456</i>	<i>1.4E-04</i>
10	0.771	3.6E-14	0.727	4.9E-12	0.407	6.8E-04	<i>0.454</i>	<i>1.5E-04</i>
11	0.772	3.1E-14	0.730	3.6E-12	0.408	6.8E-04	<i>0.447</i>	<i>1.9E-04</i>
12	0.773	2.8E-14	0.733	2.7E-12	0.409	6.5E-04	<i>0.441</i>	<i>2.5E-04</i>
13	0.774	2.5E-14	0.736	1.9E-12	0.409	6.5E-04	<i>0.444</i>	<i>2.2E-04</i>
14	0.775	2.2E-14	0.740	1.2E-12	0.407	6.9E-04	<i>0.440</i>	<i>2.6E-04</i>
15	0.776	2.0E-14	0.743	8.7E-13	0.407	6.9E-04	<i>0.435</i>	<i>3.0E-04</i>
16	0.777	1.8E-14	0.747	6.1E-13	0.407	7.0E-04	<i>0.430</i>	<i>3.6E-04</i>
17	0.777	1.6E-14	0.750	4.4E-13	0.407	7.0E-04	<i>0.427</i>	<i>3.9E-04</i>
18	0.778	1.5E-14	0.753	3.1E-13	0.407	7.0E-04	<i>0.422</i>	<i>4.7E-04</i>
19	0.778	1.5E-14	0.755	2.5E-13	0.406	7.2E-04	<i>0.417</i>	<i>5.5E-04</i>
20	0.778	1.4E-14	0.758	1.8E-13	0.406	7.2E-04	<i>0.410</i>	<i>6.9E-04</i>
21	0.778	1.4E-14	0.760	1.4E-13	0.407	6.8E-04	<i>0.406</i>	<i>8.0E-04</i>

Table S3. Results of the correlation analysis between the average of total injection rate into Prati9 and Prati29 wells, $IN(\text{both})$, and the degree of disordering of seismic sources, ZZ , and its components, $\Delta_r, \Delta_M, \Delta_\phi$ for the phase F2. The correlation have been evaluated for $ZZ, \Delta_r, \Delta_M, \Delta_\phi$ delayed from 0 to 21 days with respect to $IN(\text{both})$. The results based on Spearman rank correlation are in italics.

Delay [days]	ZZ		Δ_r		Δ_M		Δ_ϕ	
	Corr. coef.	p-value	Corr. coef.	p-value	Corr. coef.	p-value	Corr. coef.	p-value
0	0.722	7.7E-12	0.663	1.3E-09	0.452	1.4E-04	<i>0.472</i>	<i>7.6E-05</i>
1	0.723	6.9E-12	0.667	9.9E-10	0.453	1.4E-04	<i>0.466</i>	<i>9.7E-05</i>
2	0.723	6.8E-12	0.668	8.6E-10	0.453	1.3E-04	<i>0.472</i>	<i>7.8E-05</i>
3	0.723	7.0E-12	0.670	7.8E-10	0.451	1.4E-04	<i>0.477</i>	<i>6.3E-05</i>
4	0.721	8.4E-12	0.669	8.0E-10	0.450	1.5E-04	<i>0.476</i>	<i>6.6E-05</i>
5	0.721	8.6E-12	0.671	7.1E-10	0.450	1.5E-04	<i>0.470</i>	<i>8.4E-05</i>
6	0.721	8.9E-12	0.672	6.5E-10	0.451	1.5E-04	<i>0.462</i>	<i>1.1E-04</i>
7	0.720	9.1E-12	0.673	5.9E-10	0.451	1.5E-04	<i>0.465</i>	<i>1.0E-04</i>
8	0.720	9.3E-12	0.675	5.3E-10	0.450	1.5E-04	<i>0.466</i>	<i>9.8E-05</i>
9	0.720	9.4E-12	0.676	4.7E-10	0.449	1.5E-04	<i>0.467</i>	<i>9.4E-05</i>
10	0.720	9.6E-12	0.677	4.2E-10	0.448	1.6E-04	<i>0.474</i>	<i>7.2E-05</i>
11	0.721	9.1E-12	0.679	3.7E-10	0.448	1.6E-04	<i>0.475</i>	<i>6.8E-05</i>
12	0.720	9.7E-12	0.679	3.6E-10	0.448	1.6E-04	<i>0.476</i>	<i>6.5E-05</i>
13	0.719	1.0E-11	0.681	3.2E-10	0.447	1.7E-04	<i>0.479</i>	<i>5.7E-05</i>
14	0.720	9.9E-12	0.684	2.5E-10	0.445	1.8E-04	<i>0.476</i>	<i>6.5E-05</i>
15	0.719	1.0E-11	0.685	2.2E-10	0.444	1.9E-04	<i>0.471</i>	<i>7.9E-05</i>
16	0.719	1.0E-11	0.687	1.9E-10	0.443	1.9E-04	<i>0.465</i>	<i>1.0E-04</i>
17	0.719	1.0E-11	0.688	1.7E-10	0.442	2.0E-04	<i>0.460</i>	<i>1.2E-04</i>
18	0.719	1.1E-11	0.690	1.5E-10	0.442	2.1E-04	<i>0.460</i>	<i>1.2E-04</i>
19	0.718	1.2E-11	0.691	1.4E-10	0.439	2.2E-04	<i>0.457</i>	<i>1.3E-04</i>
20	0.718	1.2E-11	0.692	1.2E-10	0.439	2.3E-04	<i>0.458</i>	<i>1.3E-04</i>
21	0.717	1.3E-11	0.693	1.2E-10	0.440	2.2E-04	<i>0.462</i>	<i>1.1E-04</i>

Table S4. Results of the correlation analysis between the average of injection rate, IN , and the degree of disordering of seismic sources, ZZ , and its components, Δ_r , Δ_M , Δ_ϕ for the phase F3. The correlation have been evaluated for ZZ , Δ_r , Δ_M , Δ_ϕ delayed from 0 to 21 days with respect to IN .

Delay [days]	ZZ		Δ_r		Δ_M		Δ_ϕ	
	Corr. coef.	p-value	Corr. coef.	p-value	Corr. coef.	p-value	Corr. coef.	p-value
0	-0.603	2.9E-02	-0.199	5.1E-01	-0.321	2.8E-01	-0.195	5.2E-01
1	-0.587	3.5E-02	-0.176	5.6E-01	-0.338	2.6E-01	-0.183	5.5E-01
2	-0.571	4.2E-02	-0.154	6.2E-01	-0.354	2.3E-01	-0.171	5.8E-01
3	-0.554	4.9E-02	-0.131	6.7E-01	-0.371	2.1E-01	-0.159	6.0E-01
4	-0.538	5.8E-02	-0.108	7.3E-01	-0.387	1.9E-01	-0.147	6.3E-01
5	-0.521	6.8E-02	-0.085	7.8E-01	-0.403	1.7E-01	-0.135	6.6E-01
6	-0.505	7.8E-02	-0.063	8.4E-01	-0.420	1.5E-01	-0.123	6.9E-01
7	-0.485	9.3E-02	-0.035	9.1E-01	-0.438	1.3E-01	-0.111	7.2E-01
8	-0.469	1.1E-01	-0.013	9.7E-01	-0.454	1.2E-01	-0.098	7.5E-01
9	-0.452	1.2E-01	0.009	9.8E-01	-0.471	1.0E-01	-0.085	7.8E-01
10	-0.436	1.4E-01	0.031	9.2E-01	-0.488	9.1E-02	-0.072	8.2E-01
11	-0.419	1.5E-01	0.052	8.7E-01	-0.502	8.1E-02	-0.060	8.4E-01
12	-0.402	1.7E-01	0.074	8.1E-01	-0.519	6.9E-02	-0.047	8.8E-01
13	-0.386	1.9E-01	0.096	7.6E-01	-0.535	5.9E-02	-0.033	9.2E-01
14	-0.369	2.1E-01	0.117	7.0E-01	-0.552	5.1E-02	-0.019	9.5E-01
15	-0.352	2.4E-01	0.139	6.5E-01	-0.567	4.3E-02	-0.006	9.9E-01
16	-0.335	2.6E-01	0.161	6.0E-01	-0.582	3.7E-02	0.007	9.8E-01
17	-0.317	2.9E-01	0.182	5.5E-01	-0.597	3.1E-02	0.020	9.5E-01
18	-0.299	3.2E-01	0.204	5.0E-01	-0.610	2.7E-02	0.032	9.2E-01
19	-0.281	3.5E-01	0.225	4.6E-01	-0.622	2.3E-02	0.043	8.9E-01
20	-0.264	3.8E-01	0.247	4.2E-01	-0.640	1.9E-02	0.058	8.5E-01
21	-0.245	4.2E-01	0.268	3.8E-01	-0.651	1.6E-02	0.069	8.2E-01

Text S2. Comparison of the results of correlation analysis for different representations of closeness of hypocenters.

One of the three conditions which we expect to play a role in linking fractures and building for-reaching pathways for fluid migration is closeness of hypocenters. This condition is parameterized by the average distance between hypocenters in the space of hypocenter coordinates transformed to equivalent dimension, Δ_r . The transformation to equivalent dimensions was necessary to make comparable all eight used parameters of seismic events: three hypocentral coordinates, three independent angles determining orientations of the T and P axes of the double-couple focal mechanisms, and two angular coordinates of hypocenters in the spherical system beginning at the open hole of injection well. The comparability enabled, in turn, estimation of the degree of disordering of seismic sources, ZZ .

Δ_r significantly correlated with the injection rate, IN , in the injection phases F1 and F2. In phase F1 Δ_r was the only one component of ZZ whose correlation with IN was significant. It was then possible to apply in this phase another representations of closeness of hypocenters and compare their correlation results with the ones obtained for Δ_r . The metrics of distances between hypocenters in original Cartesian system is Euclidean. Making use of this fact we tried correlation dimension of distances between hypocenters, D_2 , and summarized squared distances in the original (x,y,z) space, $d2$, as alternatives to Δ_r .

The correlation dimension estimate, D_2 was obtained using the integral correlation method (Grassberger & Procaccia, 1983; Lasocki & De Luca, 1998). D_2 is the slope of the straight line, which relates the number of pairs of sources whose mutual distances are smaller than a certain value of ε , with ε , in the double logarithmic scale.

The summarized squared distances in the original (x,y,z) space, $d2$ was $\sum_{i \neq k} (\mathbf{x}_i - \mathbf{x}_k)^2$ where \mathbf{x}_i is the vector of hypocenter location in the original Cartesian system of coordinates.

Unlike Δ_r , D_2 did not correlated with IN at the prescribed significance level $\alpha=0.05$. The Pearson correlation coefficient was 0.26, $p=0.26$. On the contrary $d2$ was highly correlated with IN . The Pearson correlation coefficient was 0.87, $p=4 \times 10^{-7}$. We also analyzed correlation between $d2$ and IN in phase F2, in which Δ_r significantly correlated with IN (corr. coeff. = 0.69, $p = 2 \cdot 10^{-10}$, see Main text Table 2). The Pearson correlation coefficient between $d2$ and IN was 0.63, $p = 2 \times 10^{-8}$.

The correlation results with $d2$, same as those with Δ_r , validate positively the results with Δ_r because $d2$ is the most basic measure of the total distance between hypocenters. The reason why the correlation between D_2 and IN was not ascertained were probably problems with accurate estimation of the correlation dimension of distance between hypocenters, D_2 . In many data widows we could not distinguish correctly the linear part because the saturation and depopulation regions nearly overlapped. In the below graphs we present the IN vs. correlation dimension scatterplot and two plots of the correlation integral vs. threshold distance, which exemplify the difficulties with correct estimation of the correlation dimension.

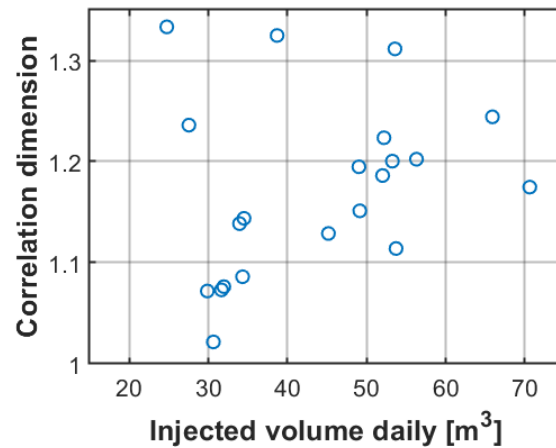


Figure Text S2-1. Scatter plot of correlation dimension of the distance between hypocenters, D_2 vs. injected volume into Prati9 well in phase F1, $IN(9)$.

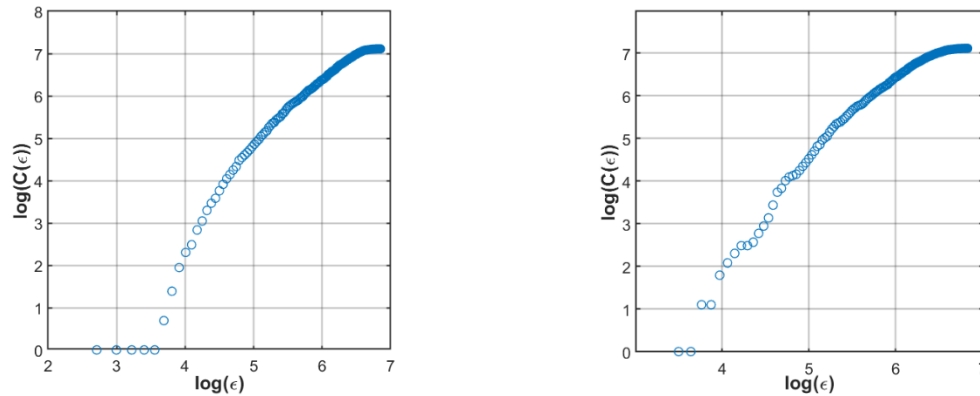


Figure Text S2-2. Two examples of the empirical relation between the correlation integral of the distance between hypocenters, $C(\varepsilon)$ and the threshold distance ε .

References:

- Grassberger, P. & Procaccia, I. (1983) Measuring of strangeness of strange attractors. *Physica D*, 9, 189–208, [https://doi.org/10.1016/0167-2789\(83\)90298-1](https://doi.org/10.1016/0167-2789(83)90298-1).
 Lasocki, S. & De Luca, L. (1998) Monte Carlo studies of relations between fractal dimensions in monofractal data sets. *Pure and Applied Geophysics*, 152, 213–220

Text S3. Discussion of the results of correlation analysis for phase F3 of injection.

In phase F3, in which the overall level of the injection rate, IN , was the lowest among injection phases, the correlation between IN , and the degree of disordering of sources, ZZ , was significant, negative. This correlation was achieved only jointly by the three components of ZZ : Δ_r , Δ_M , Δ_ϕ because neither of them significantly correlated with IN (Main text, Table 2). The negative correlation coefficient in F3 increased when ZZ was delayed with respect to IN , and for four and more days lag it became statistically not significant (Supporting Information Table S4).

The change of sign of the $IN - ZZ$ correlation in F3 may be explained by the role of injection rate changes on the weakening/strengthening of rock. According to rock sample studies of Fjaer and Ruisten (2002) in rock weakening conditions there are many equivalent orientations of the failure plane, and the fracture orientation is determined by local weaknesses of the rock. In conditions of rock strengthening only two orientations for the potential failure plane fulfil the Coulomb failure criterion. Thence rock weakening conditions result in poorly ordered seismic fractures, and in rock strengthening conditions the fractures are better ordered. Orlecka-Sikora and Cielesta (2019) found two mutually reversed reactions of the stress field to injection rate changes in The Geysers, with the reversal point at some $50\text{-}70 \cdot 10^2 \text{ m}^3/\text{day}$. At injection rates above this interval, increasing the injection rate enhanced rock weakening, and a decrease in the injection rate led to rock strengthening. Below this interval, the effect of injection rate variation was the opposite.

The injection rates in F1 and F2 were mostly above the aforementioned reversal point. To the contrary, the injection rates in F3 were well below this point. In the first two phases, weakening of the rock with increasing injection rate could favor the formation of randomly oriented fractures, which was expressed by the increase in the degree of disordering, ZZ . In F3 increasing the injection rate could lead to rock strengthening, which promoted the formation of fractures oriented in the optimal direction. As a consequence, the fractures were better ordered, which reduced ZZ .

We acknowledge, however, that since the data series in F3 was composed of only 13 points, the obtained $IN - ZZ$ correlation ($p \approx 0.03$) might be spurious.

References:

- Fjaer, E., & Ruistuen, H. (2002) Impact of the intermediate principal stress on the strength of heterogeneous rock, *Journal of Geophysical Research, Solid Earth*, 107, B2, 2032, doi: 10.1029/2001JB000277.
- Orlecka-Sikora, B. & Cielesta, S. (2019) Evidence that the injection-induced earthquakes rupture subcritically. *Scientific Reports* (revised, under review)